Supplementary information for

Heterostructured Perovskite Nanocrystals for Water Stable Plasmon-Enhanced Photoelectrocatalysis

Yuan Yuan[1+], Anastasiia P. Dmitrieva[1,2+], Stepan Pozdniakov[1,3+], Lev E. Zelenkov[1,3], Pavel Krasnov[1,4], Yangyang Ju[5], Ruslan Azizov[1,3], Ivan V. Moskalenko[6], Elena F. Krivoshapkina[2], Pavel V. Krivoshapkin[2], Pavel M. Talianov[1*], Sergey V. Makarov[1,3*], & Soslan A. Khubezhov[1*]

1. Qingdao Innovation and Development Center, Harbin Engineering University, Qingdao 266000, Shandong, China

2. EnergyLab, ITMO University, Lomonosova St. 9, Saint Petersburg, 191002, Russian Federation

3. School of Physics and Engineering, ITMO University, 49 Kronverksky pr., 197101, St. Petersburg, Russian Federation

4. International Research Center of Spectroscopy and Quantum Chemistry, Siberian Federal University, 26 Kirensky St., 660074 Krasnoyarsk, Russian Federation

5. Beijing Key Laboratory of Nanophotonics and Ultrafine Optoelectronic Systems, Advanced Research Institute of Multidisciplinary Sciences, Beijing Institute of Technology, Beijing, 100081, China

6. Infochemistry Scientific Center, ITMO University, 197101 Saint Petersburg, Russia

[+] equal contribution
* corresponding author: talyanov170195@gmail.com; s.makarov@metalab.ifmo.ru; soslan.khubezhov@gmail.com

Contents:

Materials

Lead(II) bromide ($PbBr_2$, 99.998% trace metals basis, TCI Chemicals), cesium bromide (CsBr, 99.9% trace metals basis, Sigma-Aldrich), Oleylamine (OAm, ≥98%, Sigma-Aldrich), oleic acid (OA, 90% technical grade, Sigma-Aldrich), 1-octadecene (ODE, ≥95.0% (GC), Sigma-Aldrich), cesium carbonate (Cs_2CO_3, 99.9% trace metals basis, Sigma-Aldrich), titanium(IV) butoxide (TBT, 97 %, Sigma-Aldrich), Hydrogen tetrabromoaurate(III) dihydrate, ($HAuBr_4 \cdot 2H_2O$, 99.9% trace metals basis, Sigma-Aldrich), sodium citrate ($HOC(COONa)(CH_2COONa)_2 \cdot 2H_2O$, Sigma-Aldrich), potassium hydrogen carbonate, ($KHCO_3$, 99,7%, Sigma-Aldrich), acetonitrile (CH_3CN, ≥99.9%, Sigma-Aldrich), methyl acetate (CH_3COOCH_3, 99%, Sigma-Aldrich), hexane (C_6H_{14}, ≥99.9%, Sigma-Aldrich), ethanol (EtOH, 99%, Aladdin), were used as received without additional purification. Milli-Q water with a resistance of 18.2 $M\Omega\ cm^{-1}$ was utilized for all experiments (Millipore, Bedford, MA, USA).

Synthesis of Cs-Oleate Precursor

A mixture of 407 mg of Cs_2CO_3 (1.25 mmol), 20 mL of 1-octadecene (ODE), and 1.55 mL of oleic acid (OA, 5 mmol) was added to a 50 mL, two-neck round-bottom flask under continuous stirring. The mixture was then dried at 120 °C under vacuum for 1 hour, followed by heating to 150 °C under an inert atmosphere until the complete dissolution of Cs_2CO_3. The resulting Cs-oleate solution (0.116 M) in ODE was maintained in suspension and heated until the precursor dissolved completely, prior to injection.

Synthesis of $CsPbBr_3$ nanocrystals

Nanocrystals (NCs) of $CsPbBr_3$ were synthesized via a hot-injection method[1]. In a 50 mL, three-neck round-bottom flask, 138 mg of $PbBr_2$ (0.38 mmol) and 10 mL of ODE were added and heated to 110 °C under vacuum for 1 hour. Subsequently, 1 mL of oleic acid (OA, 3.2 mmol) and 1 mL of octylamine (OAm, 3 mmol) were added dropwise under a nitrogen atmosphere. Upon complete dissolution of $PbBr_2$, the reaction mixture was further heated to 180 °C. At this stage, 0.9 mL of Cs-oleate precursor (0.116 M) was rapidly injected into the $PbBr_2$ solution in ODE, OA, and OAm. Five seconds after the injection, the reaction flask was quickly cooled using a water bath. The synthesized nanocrystals were transferred into a centrifuge tube and the excess of MA was added. Then, the crude solution was centrifuged at 5000 rpm to remove the supernatant, then nanoparticles were redissolved in n-hexane and transferred to a clean vial.

Synthesis of $CsPbBr_3@TiO_2$ core-shell nanoparticles

NCs of $CsPbBr_3$ were synthesized via the modified hot-injection method. In a 50 mL, three-neck round-bottom flask, 138 mg of $PbBr_2$ (0.38 mmol) and 10 mL of ODE were added and heated to 110 °C under vacuum for 1 hour. Subsequently, 1 mL of oleic acid (OA, 3.2 mmol) and 1 mL of octylamine (OAm, 3 mmol) were added dropwise under a nitrogen atmosphere. Upon complete dissolution of $PbBr_2$, the reaction mixture was further heated to 180 °C. At this stage, 0.9 mL of Cs-oleate precursor (0.116 M) was rapidly injected into the $PbBr_2$ solution in ODE, OA, and OAm. Afterwards, the pristine 100ul of TBT (0.29M) and 5ul of water in 2 ml of ODE for the hydrolysis reaction were added, one after the other. After these injections, the reaction flask was quickly cooled using a water bath for 10 min. The synthesized nanocrystals were transferred into a centrifuge tube and the excess of MA was added. Then, the crude solution was centrifuged at 8000 rpm to remove the supernatant, then nanoparticles were redissolved in n-hexane and transferred to a clean vial.

Synthesis of Au nanoparticles

The synthesis of colloidal gold nanoparticles (Au NPs) was carried out using the Turkevich method[2], through the reduction of hydrogen tetrabromoaurate hydrate with sodium citrate. First, 0.17 mL of a 10 wt% hydrogen tetrabromoaurate dihydrate solution was mixed with 10 mL of a 1 wt% sodium citrate solution and heated to its boiling point. The yellow solution then changed color to black and, within 2–3 minutes, transitioned to a deep wine-red hue, indicating the successful reduction of the gold ions to form Au NPs. Afterwards, the Au NP solution (3.2 mM) was redispersed by centrifugation in 10 mL of ethanol for further processing.

Scanning electron microscopy

To perform scanning electron microscopy (SEM) measurements, Au NPs *were deposited* on silicon substrate. Afterwards, SEM images were obtained with the Zeiss Crossbeam 350 microscope at the accelerating voltage of 1.5 kV. Au NPs were visualized using an in-lens detector.

Transmission electron microscopy

High-resolution transmission electron microscopy (HRTEM) images of $CsPbBr_3$ perovskite nanocrystals and $CsPbBr_3@TiO_2$ core-shell nanoparticles were acquired using a Zeiss Libra 200FE microscope, operating at an accelerating voltage of 200 kV. For HRTEM analysis, samples dispersed in hexane (1.5 µL) were deposited onto a 200-mesh copper TEM grid and dried for several minutes. Elemental mapping was performed using energy-dispersive X-ray spectroscopy (EDX) with a JEOL Centurio system. The spectra of $CsPbBr_3@TiO_2$ core–shell nanoparticles were acquired and analyzed using JEOL Analysis Station software.

X-ray diffraction

Grazing incidence X-ray diffraction (GIXRD) was performed on $CsPbBr_3$ perovskite nanocrystals and $CsPbBr_3@TiO_2$ core-shell nanoparticles deposited on a silicon substrate. The measurements were carried out using a Bruker D8 Advance diffractometer equipped with a 1.6 kW Cu-Kα radiation source (Kα1, $\lambda = 1.54059$ Å) and a parallel beam geometry. A Göbel mirror was used to produce the parallel X-ray beam required for grazing incidence measurements. Data were collected in 2θ geometry with a step size of 0.01°, a precision time of 0.3 s, and an angular resolution of 0.01° at a scanning speed of 2° min^{-1}. The incident angle was set to 1°, corresponding to an analysis depth < 100 nm.

X-ray photoelectron spectroscopy

The elemental composition and chemical state of the obtained $CsPbBr_3$ perovskite nanocrystals and $CsPbBr_3@TiO_2$ core-shell nanoparticles were studied using the X-ray photoelectron spectroscopy (XPS*)*. For XPS measurements, samples were deposited onto a silicon substrate. The analysis was performed in an ultra-high vacuum (8.6×10^{-10} mbar) using a ULVAC-PHI Genesis 900 spectrometer, equipped with a monochromatic Al-Kα X-ray source (1486.6 eV). A flood gun was employed to neutralize the surface charge, with the C 1s peak of adventitious carbon set at a binding energy (BE) of 284.8 eV. High-resolution spectra (0.1 eV resolution) were collected from a spot area of approximately 200 × 200 μm. The analyzer was operated in constant energy mode (CAE) with a pass energy of 27 eV, and 10 scans were averaged for each high-resolution spectrum. Shirley background subtraction was applied to deconvolute the spectra, and the shape of the spectral components was fitted using a 30% Gaussian/Lorentzian mixture function. The elemental atom concentrations are calculated by normalizing the curve areas of the corresponding components using the following formula:

$$\mathrm{S_{norm}} = \frac{\mathrm{S_{peak}}}{\mathrm{F_x T_x C_x}},\ \mathrm{N_{element}} = \frac{\mathrm{S_{norm}}}{\sum_{\mathrm{x}=1}^{\mathrm{n}} \mathrm{S_{norm}}}$$

where $N_{element}$ is the concentration of element x, and S_{norm} represents the normalized area under the x-element peak. Here, F_x is the sensitivity factor (orbital-dependent), T_x is the transmission function (linked to the sensitivity factor), and C_x accounts for the attenuation length, correcting for the inelastic mean free path of electrons. The parameters F_x, T_x, and C_x are derived from the Scofield libraries.

To determine the work function, a micro-focused X-ray monochromatic Al-Kα source (hv = 1486.6 eV) with a spot size of 10 μm was used. An electrostatic bias of $V_{bias} = -10$ V was applied to obtain the spectrum cutoff point. The spectra were recorded in CAE mode with a pass energy of 13 eV and a resolution of 0.05 eV. Prior to measurements, the spectrometer's energy analyzer was calibrated using a gold standard sample, with the photoemission line Au4f7 positioned at $E - E_f = 84$ eV. The work function of the sample was calculated using the formula:

$$W_{sample} = hv - (E_{cutoff} - V_{bias}),$$

where E_{cutoff} is the cutoff energy of the spectrum.

Optical measurements

Absorption spectra of Au NPs, $CsPbBr_3$ perovskite NCs and $CsPbBr_3@TiO_2$ core-shell NPs solutions were obtained using Edinburgh Instruments FS5 Spectrofluorometer.

Photoluminescence spectra and lifetime decay curves of $CsPbBr_3$ perovskite NCs and $CsPbBr_3@TiO_2$ core-shell NPs solutions were obtained using Edinburgh Instruments FLS-1000 photoluminescence spectrometer and EPL-375 picosecond laser with frequency 100 kHz. For time-resolved photoluminescence measurements data was fitted using an ABC model and bi-exponential fitting.

Initial charge carrier density was calculated according to the following equation: $n_0 = \frac{F\,Abs}{d}$, where F is a fluence, $Abs = (1-R)(1-exp(-ad))$ is a fraction of incident photons absorbed, d is a thickness of film and a is an attenuation coefficient. d was found using the Scanning Probe Microscope AIST SmartSPM by atomic force microscopy method.

Table S1. XPS Atomic concentrations for the $CsPbBr_3$ NCs and TiO_2 control samples.

Sample	Cs, %	Pb, %	Br, %	Ti. %	O, %	Au, %
$CsPbBr_3$ NCs - control	20.2	20.7	59.1			
TiO_2 - control				34.2	65.8	
$CsPbBr_3$@TiO_2	6.7	6.8	19.8	22.1	44.6	
$CsPbBr_3$@TiO_2/Au	6.3	6.5	18.7	19.9	40.5	8.1

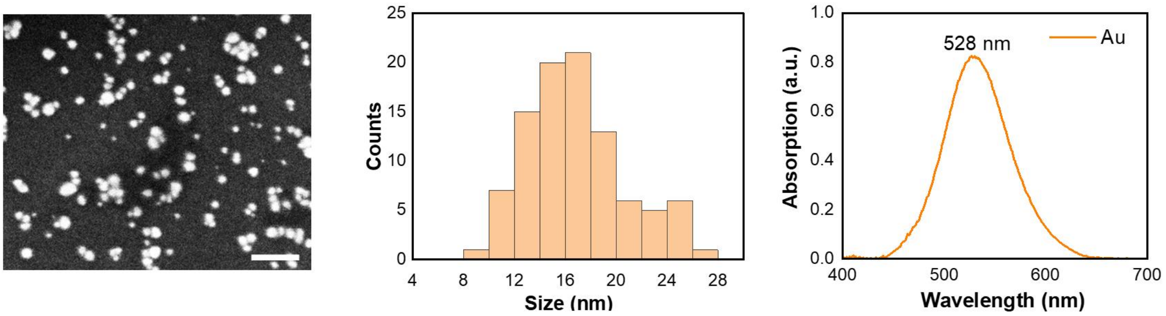

Figure S1. SEM image, particles size distribution and absorbance spectrum of Au NPs. Scale bar corresponds to 100 nm.

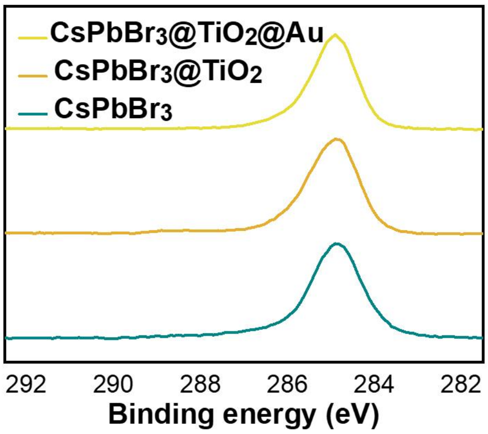

Figure S2. High-resolution C1s XPS survey spectrum for $CsPbBr_3$ NCs, $CsPbBr_3$@TiO_2 and $CsPbBr_3$@TiO_2/Au.

Table S2. XPS Atomic concentrations for the $CsPbBr_3$ and TiO_2 control samples.

Sample	Binding energy / FWHM, eV						
	Cs3d5	Pb4f7	Br3d5	Ti2p3	O1s	Au4f7	C1s
$CsPbBr_3$ NCs - control	724 1.33	138.1 1.15	68 1.2				284.85 1.25
TiO_2 - control				458.53 1.43	530.2 1.33		284.83 1.3
$CsPbBr_3$@TiO_2	724.1 1.75	138.2 1.18	68.1 1.23	458.36 1.7	530 1.36		284.87 1.19
$CsPbBr_3$@TiO_2/Au	724.2 1.74	138.3 1.17	68.1 1.26	458.81 1.67	530.4 1.48	83.8 1.1	284.9 1.27

Electron Paramagnetic Resonance Spectroscopy

Spinscan X (Adani Linev, Belarus) was used to measure the EPR spectra; the field center was 336 mT, the modulation frequency was 150 kHz, the modulation amplitude was 2 G, and the microwave power attenuation was 10 mW in glass ampoules with an internal diameter of ~ 1 mm. 5,5-dimethyl-1-pyrroline N-oxide (DMPO) was used as a trapping agent.

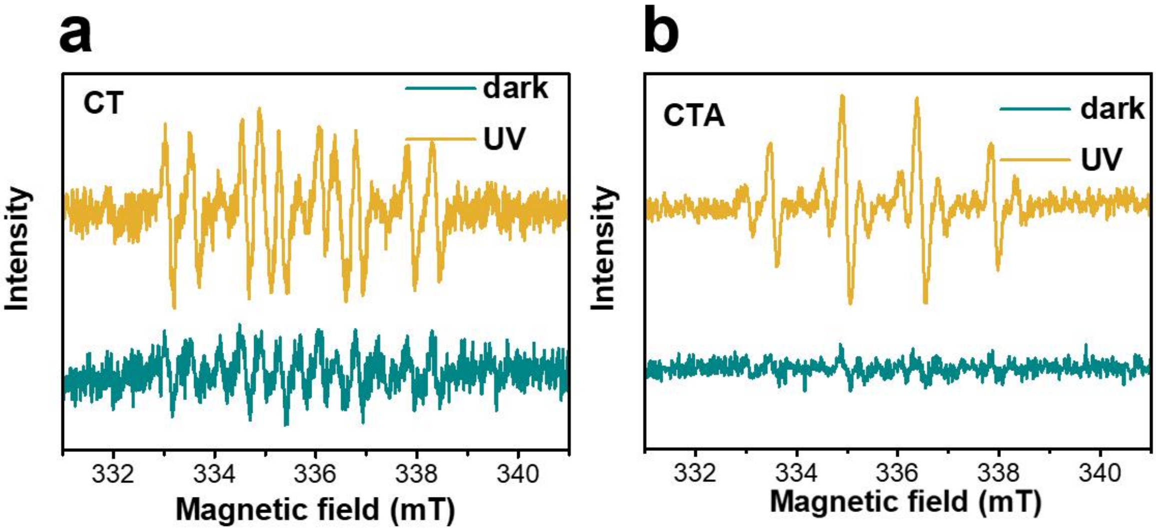

Figure S3. EPR spectra of (a) CsPbBr$_3$@TiO$_2$ (CT) and (b) CsPbBr$_3$@TiO$_2$/Au (CTA) in aqueous DMPO solution under dark and UV illumination (λ = 360 nm). Under UV light, CT shows mixed DMPO–•OH and DMPO–O_2^- signals, while CTA predominantly exhibits DMPO–•OH, indicating stronger hole oxidation and supporting the S-scheme/Schottky mechanism.

Table S3. Coefficients obtained from lifetime decay of $CsPbBr_3$ NCs and $CsPbBr_3@TiO_2$ calculated using the ABC model with the same fluence.

Sample	Fluence, photons•cm^{-2}	n_0, cm^{-3}	t, ns	A, s^{-1}	B, cm^3/s
$CsPbBr_3$ NCs	$2.5 \cdot 10^{14}$	$2.7 \cdot 10^{17}$	31.5	$3.2 \cdot 10^{7}$	$2.6 \cdot 10^{-10}$
$CsPbBr_3@TiO_2$		$1.1 \cdot 10^{17}$	17.4	$5.7 \cdot 10^{7}$	$5.7 \cdot 10^{-10}$
TiO_2		$1.2 \cdot 10^{17}$	by bi-exponential fitting (Table S4)		

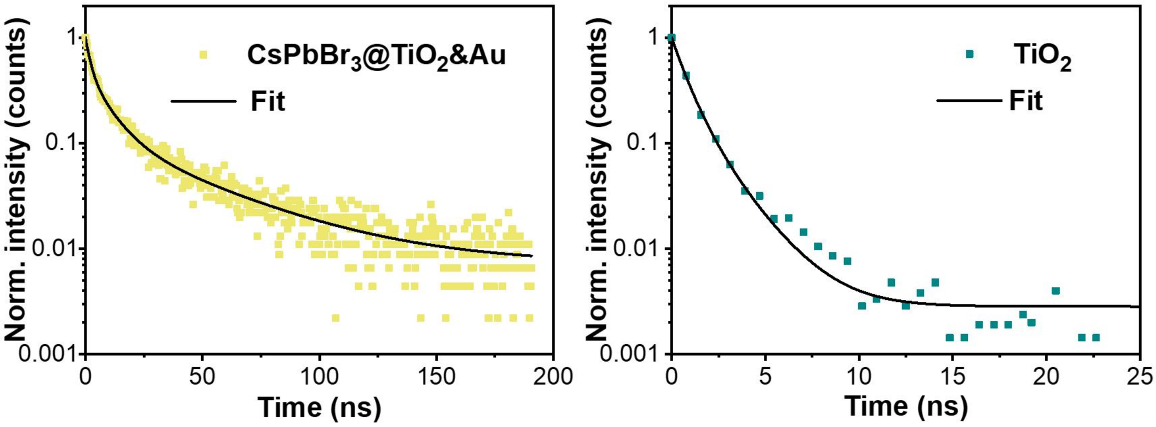

Figure S4. PL lifetime decay of $CsPbBr_3@TiO_2$/Au NPs and TiO_2 NPs layered structure.

Table S4. The bi-exponential fitting parameters of time-resolved PL decay curves for $CsPbBr_3@TiO_2$/Au NPs and TiO_2 NPs.

Sample	A_1, %	A_2, %	t_1, ns	t_2, ns	$t_{Average}$, ns
$CsPbBr_3@TiO_2$/Au	60.3	39.7	2.3	14.5	12.1
TiO_2	8.9	91.1	3.6	0.8	1.7

Bi-exponential fitting:

$$n(t) = A_1 exp(-\frac{t}{t_1}) + A_2 exp(-\frac{t}{t_2}) + C$$

where A_1, A_2 are constants, t is time, t_1, t_2 represent the decay lifetimes. The average lifetime was calculated as:

$$t_{Average} = \frac{A_1 t_1^2 + A_2 t_2^2}{A_1 t_1 + A_2 t_2}$$

Photoelectrochemical impedance spectroscopy (EIS) and ***transient photocurrent*** (TPC) measurements were performed using a VIONIC potentiostat/galvanostat (Metrohm Autolab) powered by INTELLO software. A three-electrode configuration was employed, consisting of a working electrode (catalyst-coated ITO), a Pt wire counter electrode, and an Ag/AgCl reference electrode. The measurements were conducted in 0.5 M $KHCO_3$ electrolyte, and the photoelectrochemical cell was irradiated using a xenon lamp source (HPX-2000, Ocean Insight) via a fiber optic light guide.

EIS measurements were carried out under both dark and illuminated conditions in the frequency range of 100 kHz to 0.1 Hz using a sinusoidal perturbation of 10 mV at a fixed bias of –0.7 V vs. Ag/AgCl. Transient photocurrent responses were measured under chopped light illumination to evaluate the photoinduced charge separation efficiency.

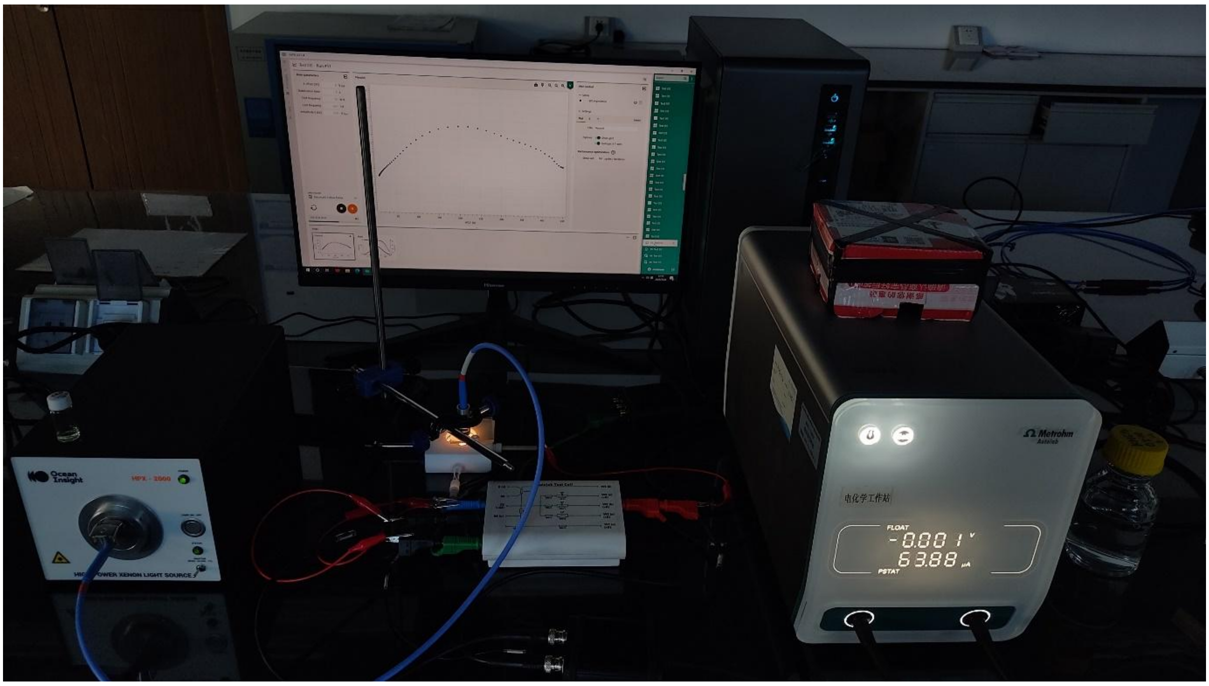

Figure S5. Setup for TPC and EIS measurements of $CsPbBr_3$ NPs, CT and CTA samples.

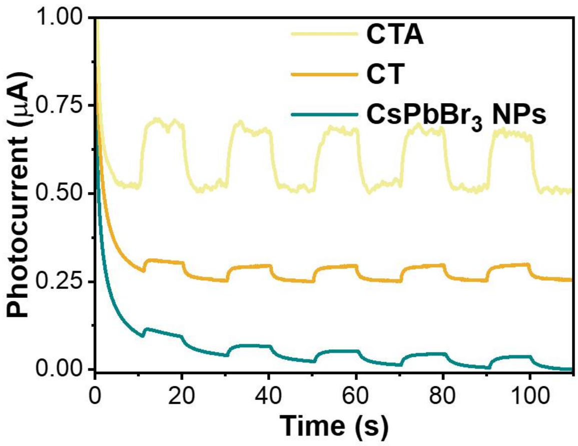

Figure S6. Photocurrent plots of $CsPbBr_3$ NPs, CT and CTA samples.

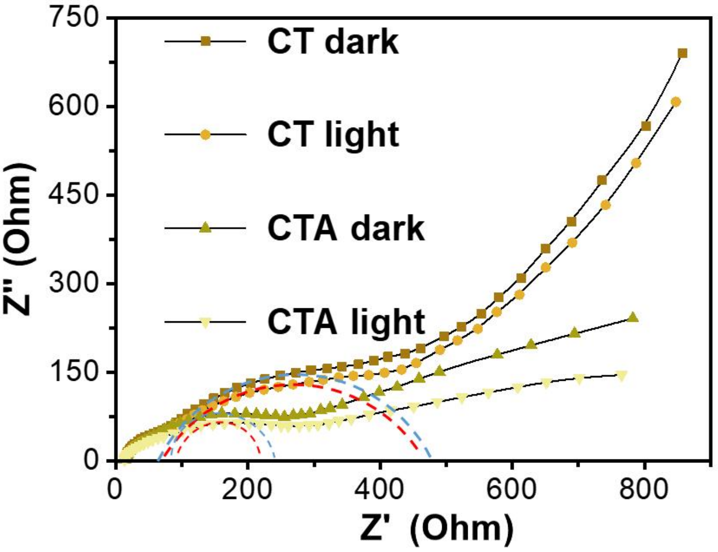

Figure S7. Nyquist plots of CT and CTA samples measured under dark and illuminated conditions.

Catalytic properties evaluation

Catalyst preparation: The catalyst was introduced to the copper foam through a process of impregnation in a $CsPbBr_3@TiO_2$ NPs solution for a duration of 24 hours. The quantification of the catalyst deposition density was ascertained utilizing a gravimetric method, yielding a measurement of 10 mg of catalyst per 1 cm^2 of the substrate. The $CsPbBr_3@TiO_2/Au$ specimens were synthesized by sequentially impregnating the substrate initially in a colloidal gold solution for a period of 24 hours, followed by impregnation in a $CsPbBr_3@TiO_2$ solution. Further, copper foam was utilized as an electrode.

Electrochemical measurements were performed using a computer-controlled electrochemical workstation (Biologic SP-200). Cyclic voltammetry experiments were carried out in a three-electrode cell equipped **(Figure S8)**, Pt carbon anode, and Ag/AgCl electrode. Solutions of 0.1M TBABr in CH_3CN and 0.5M $KHCO_3$ (40 ml) were used as electrolytes in CV and CA experiments. Before each experiment the catholyte was saturated with CO_2 (99.999%) by continuously bubbling the gas at 60 ml min^{-1} for 20 min, and the solution headspace kept under a positive pressure of a corresponding gas (CO_2) during the cyclic voltammetry measurements to eliminate the presence of oxygen in the solution. Chronoamperometric experiments were performed in the same electrochemical cell as described above. CO_2 was continuously bubbled through the reaction mixture at the rate of 60 ml min^{-1}. The gas composition in the headspace of the cell was analyzed using in-line gas chromatography analysis every 20 min until the completion of the reaction.

Photochemical measurements were performed using quartz photochemical cell **(Figure S8)** with 0.5M $KHCO_3$ (40 ml) used as an electrolyte. Excitation source wavelength and power density corresponded to 300-400 nm and 1.4 W m^{-2}. A solution of $KHCO_3$ was irradiated (400 nm) under CO_2 bubbling at the rate 60 ml min^{-1}. The gas composition in the headspace of the cell was analyzed using in-line gas chromatography analysis every 20 min until the completion of the reaction.

Photoelectrochemical measurements were performed using quartz photochemical three electrode cell **(Figure S8)** equipped, Pt carbon anode, and Ag/AgCl electrode with 0.5M $KHCO_3$ (40 ml) used as an electrolyte. Excitation source wavelength and power density corresponded to 300-400 nm and 1.4 W m^{-2}. Prior to the initiation of each experimental trial, the catholyte underwent saturation with carbon dioxide (99.999%) through the continuous infusion of the gas at a flow rate of 60 ml min^{-1} for a duration of 20 minutes, while concurrently maintaining the solution headspace under a positive pressure of the corresponding gas (CO_2) throughout the cyclic voltammetry assessments to mitigate the presence of oxygen in the solution. Chronoamperometric investigations were conducted utilizing the identical electrochemical cell as previously delineated. Carbon dioxide was perpetually bubbled through the reaction mixture at a specified rate of 60 ml min^{-1}. The gas composition within the headspace of the cell was meticulously analyzed utilizing in-line gas chromatography at 20-minute intervals until the reaction reached completion.

Figure S8. Electrochemical cell.

References

1. Protesescu, L. et al. Nanocrystals of cesium lead halide perovskites ($CsPbX_3$, X = Cl, Br, and I): novel optoelectronic materials showing bright emission with wide color gamut. *Nano Letters* **15**, 3692-3696 (2015) doi: 10.1021/nl5048779.
2. Nasir, S. M. & Nur, H. Gold nanoparticles embedded on the surface of polyvinyl alcohol layer. *Journal of Fundamental Sciences* **4**, 245-252 (2008) doi: 10.11113/mjfas.v4n1.33.